Landing Autopilot for the Control of Airplane by Using the H-inf Control

Mihai Lungu and Romulus Lungu

Abstract—**The paper focuses on automatic control of airplane in longitudinal and lateral-directional planes, during landing, by using the linearized dynamics of airplane and the H-inf control; both planes (longitudinal and lateral-directional) are treated; the new obtained automatic landing system will consist of three subsystems: the first two control airplane's motion in longitudinal plane, while the third one is used for the control of airplane motion in lateral-directional plane. The theoretical results are validated through numerical simulations for a Boeing 747 airplane.**

Index Terms—**Landing, autopilot, H-inf control.**

I. INTRODUCTION

During landing (most difficult stage of flight), the airplanes have to perform a precise maneuver in the proximity of the ground to land safely at a suitable touch point with acceptable sink rate, speed, and attitude [1]. There are many methods to design automatic landing systems (ALSs); for the control of the lateral motion during landing, an Instrumental Landing System (ILS) type radio-navigation system together with a system used for the obtaining of distances between the airplane and the runway radio-markers has been used in [2], [3]. The direction controllers which are used within such ALSs can be PD, PI, or PID type, in classical or fuzzy variants [4] etc. In the research area of optimal synthesis, Ochi and Kanai have used the H-inf control technique to design airplanes' automatic approach and landing [5], but the authors did not analyze the robustness of the designed controllers in the presence of sensor errors and wind shears. The usage of different adaptive control architectures such as the ones based on the dynamic inversion technique and neural networks (NNs), with or without Pseudo Control Hedging blocks [6] is motivated by the presence of known nonlinearities associated to the dynamics of airplane or actuators as well as to the external disturbances. In [7] some feed-forward neural networks based on the back propagation learning algorithm have been used, but their main disadvantage is related to the priori training on normal and faulty operating data. The main disadvantages of the NN based approaches designed in [8, 9] are the required operating conditions which are not easy to satisfy in practical control applications. On the other hand, the main drawback of all the papers dealing with airplane landing is that the designed ALSs are designed either

for the longitudinal plane or for the lateral-directional plane. The present work focuses on airplane automatic control in the two planes, during landing, by using the H-inf control. Our aim is to design a new landing control system (both planes) which cancels the negative effect of possible disturbances (wind shears, crosswind, or errors of the sensors).

II. CONTROL OF THE AIRPLANE IN LONGITUDINAL PLANE

The landing procedure involves three main phases: initial approach, glide slope, and flare [10]. The initial approach means the descent of airplane from the cruise altitude to approximately 420 m above the ground. During next two stages, the speed and pitch angle must be controlled; as airplane descends to 7-20 m (the maximum value is for Boeing 747), the slope angle control system is disengaged and a flare maneuver is executed [11]. The vertical descent rate is slightly decreased such that the landing gear may be able to dissipate the energy of the impact at landing. The pitch angle of the airplane is then adjusted, between 0 to 5 degrees to allow a soft touchdown on the runway surface [12]. These issues will be achieved by the first two systems presented in this paper − the ones for the control of airplane's trajectory in the longitudinal plane. Airplane motion in lateral plane should be done without errors, this meaning the cancel of airplane's deviation with respect to the runway direction; for this, there will be designed the third system presented in this work − the one for the control of airplane trajectory in the lateral- directional plane. In Fig. 1, there are presented the main elements of airplane's geometry with respect to the runway − longitudinal and lateral-directional planes; in Fig. 1, PA is the glide slope, PDA − the runway, γ_c − the imposed slope angle of the trajectory, R − the distance between airplane and the radio-marker, γ − the slope angle, Y − the airplane lateral deviation with respect to runway, $\overline{\psi}$ − the runway direction, ψ − the flight direction, β − the glide slope angle. The expression of the angle Γ is [13]:

$$\Gamma = \frac{1}{R}\int_0^t V\Gamma' d\tau = \frac{1}{R}\int_0^t V(\gamma_c - \gamma)d\tau \cong \frac{V_0}{R}\int_0^t V(\gamma_c - \gamma)d\tau. \quad (1)$$

The linearized dynamics used in this paper for airplane's motion in longitudinal plane belongs to a Boeing 747 [13]:

$$\dot{x} = Ax + Bu, \, y_e = Cx, \quad (2)$$

with $x \in R^{6\times1}$ − the state vector, $x = \begin{bmatrix} V_x & V_z & \omega_y & \theta & \delta_p & \delta_T \end{bmatrix}^T$ and $u = \begin{bmatrix} \delta_{p_c} & \delta_{T_c} \end{bmatrix}^T$ − the control input vector; V_x is the longitudinal velocity, V_z − the vertical velocity, ω_y − the pitch angular rate,

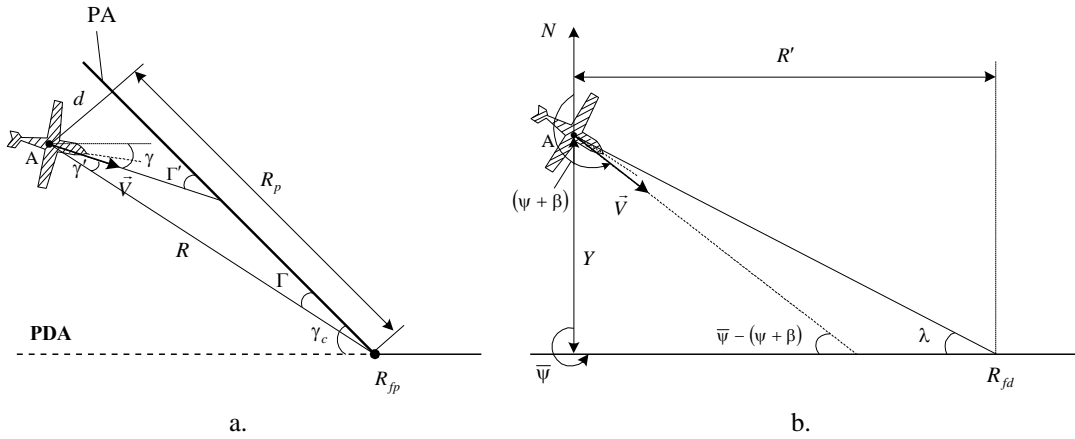θ – the pitch angle, while δ_p and δ_T are the elevator and the

Fig. 1. The geomtery of motions: a) longitudinal plane; b) lateral-directional plane.

by the equations: $T_p\dot{\delta}_p + \delta_p = \delta_{p_c}$ and $T_T\dot{\delta}_T + \delta_T = \delta_{T_c}$; T_p, T_T are the elevator and engine's time constants. The forms of the matrices A and B are [13]:

$$A = \begin{vmatrix} a_{11} & a_{12} & a_{13} & a_{14} & b_{11} & b_{12} \\ a_{21} & a_{22} & a_{23} & a_{24} & b_{21} & b_{22} \\ a_{31} & a_{32} & a_{33} & a_{34} & b_{31} & b_{32} \\ 0 & 0 & 1 & 0 & 0 & 0 \\ 0 & 0 & 0 & 0 & -\dfrac{1}{T_p} & 0 \\ 0 & 0 & 0 & 0 & 0 & -\dfrac{1}{T_T} \end{vmatrix}, B = \begin{vmatrix} 0 & 0 \\ 0 & 0 \\ 0 & 0 \\ 0 & 0 \\ \dfrac{1}{T_p} & 0 \\ 0 & \dfrac{1}{T_T} \end{vmatrix}; \quad (3)$$

the output vector is chosen as: $y_e = \begin{bmatrix} V_x & \gamma \end{bmatrix}^T$; $\gamma = \theta - \alpha = \theta - \dfrac{1}{V_0} V_z$, where $V_0 \cong V_{x_0}$ is the nominal value of the airplane's forward velocity.

To control the longitudinal velocity V_x and the slope angle γ (to control the angle Γ), one introduces the state vector:

$$x_c = \begin{bmatrix} x_{c_1} & x_{c_2} & x_{c_3} \end{bmatrix}^T = \begin{bmatrix} \dfrac{1}{Ts+1}(\bar{V}_x - V_x) & \dfrac{V_0}{s}(\gamma_c - \gamma) & \dfrac{1}{s}(\bar{\Gamma} - \Gamma) \end{bmatrix}^T,$$

where $\bar{V}_x, \gamma_c, \bar{\Gamma}$ are the imposed values of the variables V_x, γ, Γ. According to the last equation, the supplementary vector $x_c = \begin{bmatrix} x_{c_1} & x_{c_2} & x_{c_3} \end{bmatrix}^T$ depends on the system's state vector, i.e. [14]: $\dot{x}_c = A_{21}x + A_{22}x_c + B_{21}u_c + B_{22}u$, with $u_c = \begin{bmatrix} \bar{V}_x & \gamma_c & \bar{\Gamma} \end{bmatrix}^T$. Taking into account the expression of y_e and the last form of (1), one obtains the expressions of $\dot{x}_{c_1}, \dot{x}_{c_2}, \dot{x}_{c_3}$. From these equations and the expression of $\dot{x}_c$, it results the matrices:

$$A_{21} = \begin{vmatrix} -\dfrac{1}{T} & 0 & 0 & 0 & 0 & 0 \\ 0 & 1 & 0 & -V_0 & 0 & 0 \\ 0 & 0 & 0 & 0 & 0 & 0 \end{vmatrix}, A_{22} = \begin{vmatrix} -\dfrac{1}{T} & 0 & 0 \\ 0 & 0 & 0 \\ 0 & -\dfrac{1}{R_0} & 0 \end{vmatrix}, B_{21} = \begin{vmatrix} \dfrac{1}{T} & 0 & 0 \\ 0 & V_0 & 0 \\ 0 & 0 & 1 \end{vmatrix}, B_{22} = \begin{bmatrix} 0 & 0 \\ 0 & 0 \\ 0 & 0 \end{bmatrix}.$$

One chooses the following output vector $z = \begin{bmatrix} z_1 & z_2 & z_3 \end{bmatrix}^T = \begin{bmatrix} c_1 x_{c_1} & c_2 x_{c_3} & c_3 \delta_{p_c} & c_4 \delta_{T_c} \end{bmatrix}^T$, where c_1, c_2, c_3 are positive constants; the vector z can be written under the form:

$$z = C_{11}x + C_{12}x_c + D_{11}u_c + D_{12}u. \quad (4)$$

By identification, there are obtained: $C_{11} = 0_{4 \times 5}$, $D_{11} = 0_{4 \times 3}$,

$$C_{12} = \begin{vmatrix} c_1 & 0 & 0 \\ 0 & 0 & c_2 \\ 0 & 0 & 0 \\ 0 & 0 & 0 \end{vmatrix}, D_{12} = \begin{vmatrix} 0 & 0 \\ 0 & 0 \\ c_3 & 0 \\ 0 & c_4 \end{vmatrix}.$$ The output vector for achieving

the airplane's control in glide slope phase is expressed as:

$$y = C_{21}x + C_{22}x_c + D_{21}u_c + D_{22}u,$$
$$C_{21} = \begin{bmatrix} I_{6 \times 6} \\ 0_{3 \times 6} \end{bmatrix}, C_{22} = \begin{bmatrix} 0_{6 \times 3} \\ I_{3 \times 3} \end{bmatrix}, D_{21} = 0_{9 \times 3}, D_{22} = 0_{9 \times 2}. \quad (5)$$

Moreover, the first equation (2) can be put under the form: $\dot{x} = A_{11}x + A_{12}x_c + B_{11}u_c + B_{12}u$, with $A_{11} = A$, $A_{12} = 0_{6 \times 3}$, $B_{11} = 0_{6 \times 3}$, $B_{12} = B$; putting together the expressions of $\dot{x}, \dot{x}_c, z$, and y, one obtains the following equation:

$$\begin{bmatrix} \dot{x} \\ \dot{x}_c \\ z \\ y \end{bmatrix} = \begin{bmatrix} A_{11} & A_{12} & | & B_{11} & \vdots & B_{12} \\ A_{21} & A_{22} & | & B_{21} & \vdots & B_{22} \\ \hline C_{11} & C_{12} & | & D_{11} & \vdots & D_{12} \\ \hline C_{21} & C_{22} & | & D_{21} & \vdots & D_{22} \end{bmatrix} \begin{bmatrix} x \\ x_c \\ u_c \\ u \end{bmatrix} = \begin{bmatrix} \bar{A} & | & B_1 & \vdots & B_2 \\ \hline C_1 & | & D_{11} & \vdots & D_{12} \\ \hline C_2 & | & D_{21} & \vdots & D_{22} \end{bmatrix} \begin{bmatrix} x \\ x_c \\ u_c \\ u \end{bmatrix}. \quad (6)$$

The control law is chosen of the following form: $u = -Ky = -\begin{bmatrix} K_1 & K_2 \end{bmatrix} \begin{bmatrix} x^T & x_c^T \end{bmatrix}^T$, $K = B_2^T P_\infty$, with $P_\infty \in R^{9 \times 9}$ – the solution of the Riccati matriceal equation [13]:

$$\bar{A}^T P_\infty + P_\infty \bar{A} + P_\infty \left[\mu^{-2} B_1 B_1^T - B_2 \left(D_{12}^T D_{12} \right)^{-1} B_2^T \right] P_\infty + C_1^T C_1 = 0, \quad (7)$$

where the constant μ must be minimized, $C_1 = \begin{bmatrix} C_{11} & C_{12} \end{bmatrix}$, $B_1 = \begin{bmatrix} B_{11}^T & B_{21}^T \end{bmatrix}^T$, $B_2 = \begin{bmatrix} B_{12}^T & B_{22}^T \end{bmatrix}^T$. The block diagram of the subsystem for glide slope phase's control is given in Fig. 2.

For the control of airplane during the flare phase, in the state vector, the altitude H is introduced; the equation associated to this new state is: $\dot{H} = -\dfrac{1}{\tau} H$. Thus, the new state vector becomes: $x = \begin{bmatrix} V_x & V_z & \omega_y & \theta & H & \delta_p & \delta_T \end{bmatrix}^T$; the matrices A and B are modified according to the expressions (3) and to the differential equation of the airplane's altitude. One has chosen as output vector – $y_e = \begin{bmatrix} V_x & V_z & \theta & H \end{bmatrix}^T$. The expression of $\dot{H}$ can be written as [13]: $\dot{H} = V_{x_0} \theta - V_z$; between the two

equations of $\dot{H}$ there is a difference (error): $e_h = \dot{H} + \dfrac{1}{\tau}H$, that must tend to an imposed value $\bar{e}_h = 0$. In order to have $e_h = \bar{e}_h$, after the deviation $\tilde{e}_h = \bar{e}_h - e_h$ one will introduce an ideal integrator on the subsystem's direct way; thus, it appears the state: $x_{c_2} = \dfrac{1}{s}\tilde{e}_h$; therefore, $x_c = \begin{bmatrix} x_{c_1} & x_{c_2} \end{bmatrix}^T$ and $u_c = \begin{bmatrix} \bar{V}_x & \bar{e}_h \end{bmatrix}^T$. As in the glide slope case, one obtains the expressions of $\dot{x}_{c_1}, \dot{x}_{c_2}$; using these, it results:

$$A_{21} = \begin{vmatrix} -\dfrac{1}{T} & 0 & 0 & 0 & 0 & 0 & 0 \\ 0 & 1 & 0 & -V_0 & -\dfrac{1}{\tau} & 0 & 0 \end{vmatrix}, A_{22} = \begin{bmatrix} -\dfrac{1}{T} & 0 \\ 0 & 0 \end{bmatrix}, B_{21} = \begin{bmatrix} \dfrac{1}{T} & 0 \\ 0 & 1 \end{bmatrix}, B_{22} = 0_{2\times2}.$$

One chooses the output vector z (verifying (4)) of the form:

$$z = \begin{bmatrix} z_1 & z_2 & z_3 \end{bmatrix}^T = \begin{bmatrix} c_1 x_{c_1} & c_2 x_{c_2} & c_3 \delta_{p_c} & c_4 \delta_{T_c} \end{bmatrix}^T, \qquad (8)$$

with $C_{11} = 0_{4\times7}, D_{11} = 0_{4\times2}, C_{12} = \begin{vmatrix} c_1 & 0 \\ 0 & c_2 \\ 0 & 0 \\ 0 & 0 \end{vmatrix}, D_{12} = \begin{vmatrix} 0 & 0 \\ 0 & 0 \\ c_3 & 0 \\ 0 & c_4 \end{vmatrix}$; the output vector y is: $y = \begin{bmatrix} x^T & x_c^T \end{bmatrix}^T = \begin{bmatrix} V_x & V_z & \omega_y & \theta & H & \delta_p & \delta_T & x_{c_1} & x_{c_2} \end{bmatrix}^T$, that can be put under form (5) with $C_{21} = \begin{vmatrix} I_{7\times7} \\ 0_{2\times7} \end{vmatrix}, C_{22} = \begin{vmatrix} 0_{7\times2} \\ I_{2\times2} \end{vmatrix}$, $D_{21} = 0_{9\times2}, D_{22} = 0_{9\times2}$. Also, in this case, $A_{11} = A, A_{12} = 0_{7\times2}$, $B_{11} = 0_{7\times2}, B_{12} = B$. The control law is calculated as above. The block diagram of the subsystem for flare phase's control is presented in Fig. 3.

III. AIRPLANE'S CONTROL IN LATERAL-DIRECTIONAL PLANE

Before start of the landing two main stages in longitudinal plane, the pilot must cancel the airplane's lateral deviation with respect to the runway (lateral-directional plane); for this, the next subsystem of the new designed ALS will be used [1]; two commands (rudder and ailerons' commands) are necessary.

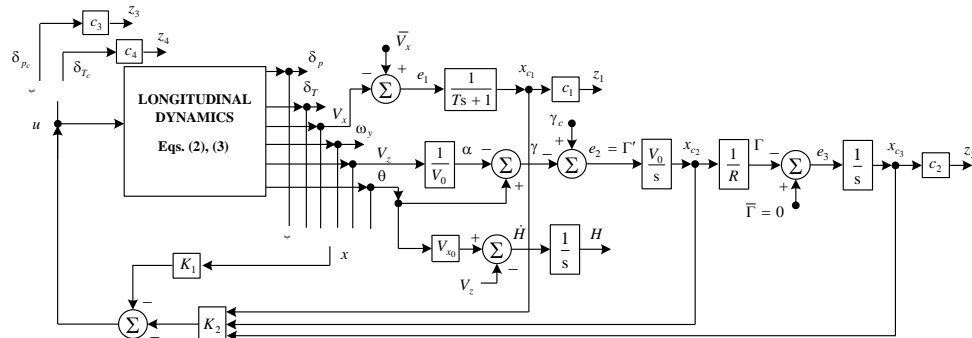The state vector and the command vector of the system

Fig. 2. Airplane control subsystem during glide slope phase (longitudinal plane).
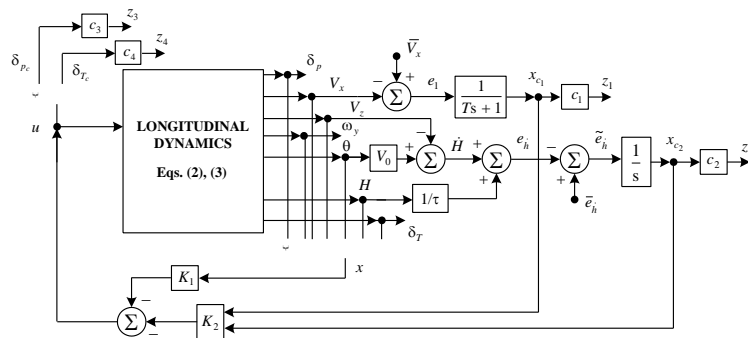

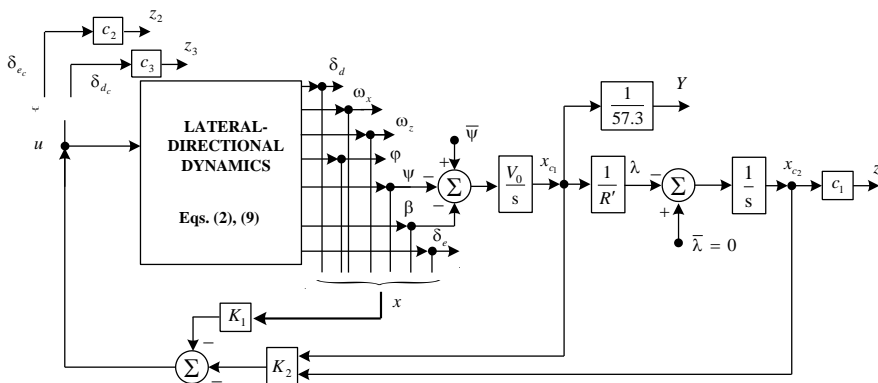Fig. 3. Airplane control subsystem during flare phase (longitudinal plane).

Fig. 4. Airplane control subsystem during initial approach (lateral-directional plane).

are: $x = \begin{bmatrix} \beta & \omega_x & \omega_z & \varphi & \psi & \delta_e & \delta_d \end{bmatrix}^T$, $u = \begin{bmatrix} \delta_{e_c} & \delta_{d_c} \end{bmatrix}^T$, where δ_e (ailerons' command) and δ_d (rudder's command) verify the equations: $T_e \dot{\delta}_e + \delta_e = \delta_{e_c}$, $T_d \dot{\delta}_d + \delta_d = \delta_{d_c}$; φ and ψ are the roll and yaw angles, while ω_x and ω_z are the roll and yaw angular rates, respectively. With these, the matrices A and B from airplane's dynamics are, respectively:

$$A = \begin{bmatrix} a_{11} & a_{12} & a_{13} & a_{14} & 0 & b_{11} & b_{12} \\ a_{21} & a_{22} & a_{23} & a_{24} & 0 & b_{21} & b_{22} \\ a_{31} & a_{32} & a_{33} & 0 & 0 & b_{31} & b_{32} \\ 0 & 1 & 0 & 0 & 0 & 0 & 0 \\ 0 & 0 & 1 & 0 & 0 & 0 & 0 \\ 0 & 0 & 0 & 0 & 0 & -\dfrac{1}{T_e} & 0 \\ 0 & 0 & 0 & 0 & 0 & 0 & -\dfrac{1}{T_d} \end{bmatrix}, B = \begin{bmatrix} 0 & 0 \\ 0 & 0 \\ 0 & 0 \\ 0 & 0 \\ 0 & 0 \\ \dfrac{1}{T_e} & 0 \\ 0 & \dfrac{1}{T_d} \end{bmatrix}; \quad (9)$$

the supplementary state vector is chosen of the form [13]:

$$x_c = \begin{bmatrix} x_{c_1} & x_{c_2} \end{bmatrix}^T = \begin{bmatrix} \dfrac{V_0}{s}(\overline{\psi} - \psi - \beta) & \dfrac{1}{s}(\overline{\lambda} - \lambda) \end{bmatrix}^T, \quad (10)$$

such that, in stationary regime, one gets: $\psi + \beta = \overline{\psi}$ and $\lambda = \overline{\lambda} = 0$. One obtains the expressions of $\dot{x}_{c_1}, \dot{x}_{c_2}$; using these, it results: $A_{21} = \begin{bmatrix} -V_0 & 0 & 0 & 0 & -V_0 & 0 & 0 \\ 0 & 0 & 0 & 0 & 0 & 0 & 0 \end{bmatrix}$, $A_{22} = \begin{bmatrix} 0 & 0 \\ -\dfrac{1}{R'} & 0 \end{bmatrix}$,

$B_{21} = \begin{bmatrix} V_0 & 0 \\ 0 & 1 \end{bmatrix}$, $B_{22} = 0_{2 \times 2}$. The form of the output vector is $z = \begin{bmatrix} z_1 & z_2 & z_3 \end{bmatrix}^T = \begin{bmatrix} c_1 x_{c_2} & c_2 \delta_{e_c} & c_3 \delta_{d_c} \end{bmatrix}^T$; z verifies (4) with

$C_{11} = 0_{3 \times 7}$, $D_{11} = 0_{3 \times 2}$, $C_{12} = \begin{bmatrix} 0 & c_1 \\ 0 & 0 \\ 0 & 0 \end{bmatrix}$, $D_{12} = \begin{bmatrix} 0 & 0 \\ c_2 & 0 \\ 0 & c_3 \end{bmatrix}$; the vector y

for control is: $y = \begin{bmatrix} x^T & x_c^T \end{bmatrix}^T = \begin{bmatrix} \beta & \omega_x & \omega_z & \varphi & \psi & \delta_e & \delta_d & x_{c_1} & x_{c_2} \end{bmatrix}^T$;

it verifies the first equation (5) with $C_{21} = \begin{bmatrix} I_{7 \times 7} \\ 0_{2 \times 7} \end{bmatrix}$, $C_{22} = \begin{bmatrix} 0_{7 \times 2} \\ I_{2 \times 2} \end{bmatrix}$,

$D_{21} = 0_{9 \times 2}$, $D_{22} = 0_{9 \times 2}$. Using these, the matrices from (6) are obtained; these are used to the obtaining of the matrix K as function of $P_\infty \in R^{9 \times 9}$ – solution of the Riccati equation (7). The block diagram of the subsystem for the control of airplane in lateral-directional plane is presented in Fig. 4.

IV. NUMERICAL SIMULATION RESULTS

To study the performances of the new obtained automatic landing system (having three subsystems – two for the control in longitudinal plane (Figs. 2 and 3) and one for the control in lateral-directional plane – Fig. 4), we consider the landing of a Boeing 747 airplane. Complex simulations in Matlab/Simulink environment have been performed. For the longitudinal plane, the values of the coefficients from the block diagram in Fig. 2 are [15]: $V_0 = 67\,\text{m/s}, c_1 = 60, c_2 = 400, c_3 = c_4 = 10, \mu = 5.1 \cdot 10^{-4}$, $\begin{bmatrix} \overline{V}_x & \gamma_c & \overline{\Gamma} \end{bmatrix}^T = \begin{bmatrix} V_0 & -2.5° & 0 \end{bmatrix}^T, H_p = H(0) = 60\,\text{m}, x_p = x(0) = 0, R_0 = 1800\,\text{m}, x_{c_1}(0) = x_{c_2}(0) = x_{c_3}(0) = 0\,\text{m}$; for the flare phase (the subsystem in Fig. 3), one used the values [13, 15]: $T = 0.01\,\text{s}$, $\tau = 6\,\text{s}, H_0 = 20\,\text{m}, c_1 = 900, c_2 = c_3 = 20, c_4 = 600, \begin{bmatrix} \overline{V}_x & \overline{e}_h \end{bmatrix}^T = \begin{bmatrix} 67\,\text{m/s} & 0\,\text{m/s} \end{bmatrix}^T, \mu = 0.107, R' = 6000\,\text{m}$. In Fig. 5 one represents the time characteristics for the glide slope and flare phases, respectively. The time origin for the flare trajectory is chosen zero when the altitude is $H = H_0 = 20$ m (altitude at which the glide slope phase ends). One may remark in Fig. 5 that the slope angle is in perfect accord with its desired values: -2.5 degrees during glide slope phase and 0 degrees during flare, respectively. During the glide slope landing phase, the airplane describes a linear descendent trajectory (9th graphic in Fig. 5.a), while in the flare phase, it describes a parabolic trajectory (9th graphic in Fig. 5.b) with a null slope angle.
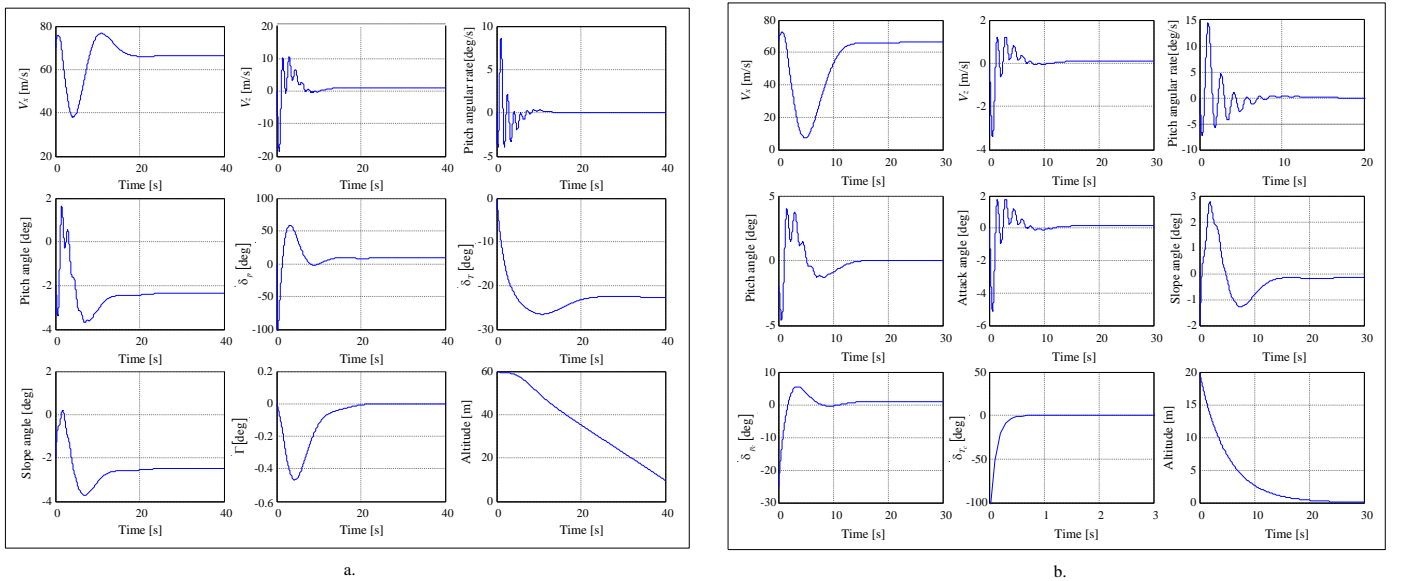

a.

b.

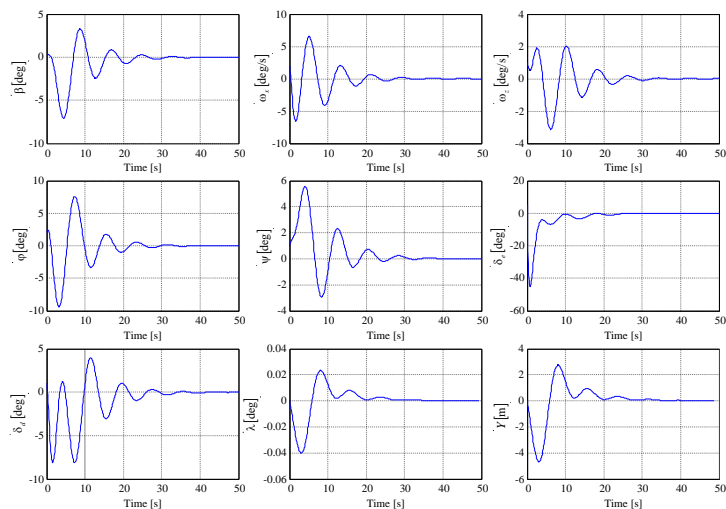Fig. 5. Time characteristics for the longitudinal plane: a) glide slope phase; b) flare phase.

Fig. 6. Time characteristics for the lateral-directional plane.

For lateral-directional plane, the coefficients from Fig. 4 are [15]: $V_0 = 67\,\text{m/s}, T_e = T_d = 2.1\text{s}, c_1 = 650, c_2 = c_3 = 1, \mu = 7, \left[\overline{\psi} \;\; \overline{\lambda}\right]^{\text{T}} = \left[0 \;\; 0\right]^{\text{T}},$ $x(0) = \left[0.5\,\text{grd} \;\; 2\,\text{grd/s} \;\; 1\,\text{grd/s} \;\; 2\,\text{grd} \;\; 1\,\text{grd} \;\; 5\,\text{grd} \;\; 1\,\text{grd}\right]^{\text{T}}$. The time characteristics associated to the initial approach phase are presented in Fig. 6; it can be observed that the subsystem responds very well and the lateral deviation of the airplane with respect to the runway line is cancelled $(Y \to 0)$.

V. Conclusion

In this paper, one designed an ALS using the H-inf technique; it consists of three landing subsystems that have been software implemented, and validated; the first two subsystems are useful for landing control in longitudinal plane (glide slope and flare), while the third one is used in lateral plane. The advantage is the applicability to problems involving multivariate systems with cross-coupling between channels. The whole system has been software implemented, tested, and validated through numerical simulations; promising results have been obtained.

References

[1] R. Lungu and M. Lungu, *Airplane Landing Control Using the H-inf Control and the Dynamic Inversion Technique*, Intech Publisher, pp. 101-120, 2016.

[2] M. Lungu, *Flight Control Systems (Sisteme de Conducere a Zborului)*, Sitech Publisher, Craiova, 2008.

[3] D. McLean, *Automatic Flight Control Systems*, Prentice Hall Publisher, 1990.

[4] L. Zhi and W. Yong, "Intelligent landing of unmanned aerial vehicle using hierarchical fuzzy control," *IEEE Aerospace Conference*, pp. 1-12, 2012.

[5] Y. Ochi and K. Kanai, "Automatic approach and landing for propulsion controlled airplane by H-inf control," *IEEE International Conference on Control Applications*, Hawaii, pp. 997-1002, 1999.

[6] A. Calise, E. Johnson, M. Johnson, and J. Corban, "Applications of adaptive neural - Networks control to unmanned aerial vehicles," *Journal of Harbin Institute of Technology*, vol. 38, no. 11, pp. 1865-1869, 2006.

[7] T. Wagner and J. Valasek, "Digital Autoland Control Laws Using Quantitative Feedback Theory and Direct Digital Design", *Journal of Guidance, Control, and Dynamics*, vol. 30, no. 5, pp. 1399-1413, 2007.

[8] J. Jang and G. Jeon, "A parallel neuro-controller for DC motors containing nonlinear friction," *Neurocomputing*, vol. 30, pp. 233-248, 2000.

[9] S. Seshagiri and H. K. Khalil, "Output feedback control of nonlinear systems using RBF neural network," *IEEE Transactions on Neural Networks*, vol. 11, pp. 69-79, 2000.

[10] B. Parkinson, M. O'Connor, and K. Fitzgibbon, "Airplane automatic approach and landing using GPS," *Global Positioning System: Theory and Applications*, vol. II, pp. 397-425, 1996.

[11] R. Lungu and M. Lungu, "Application of H_2/H_∞ and dynamic inversion techniques to airplane landing control," *Aerospace Science and Technology*, vol. 46, no. 1, pp. 146-158, 2015.

[12] J. Juang, H. Chang, and W. Chang, "Intelligent automatic landing system using time delay neural network controller," *Applied Artificial Intelligence: An International Journal*, vol. 17, no. 7, pp. 563-581, 2003.

[13] R. Lungu and M. lungu, "Airplane automatic control during landing (Controlul automat al aeronavelor la aterizare). Sitech Publisher, 2015.

[14] O. Yashimaso and K. Kimio, "Automatic Approach and Landing for propulsion controlled airplane by H-inf control," in *Proc. the IEEE International Conference on Control Applications*, Hawaii, pp. 997-1002, 1999.

[15] R. Lungu, M., Lungu, and T. L. Grigorie, "ALSs with conventional and fuzzy controllers considering wind shears and gyro errors," *Journal of Aerospace Engineering*, vol. 26, no. 4, pp. 794-813, 2012.

Mihai Lungu was born in Craiova, Romania, in 1980. In 2004 he graduated the University of Craiova, Faculty of Electrical Engineering, Specia- lization: Board Equipments and Devices. In 2008 he received the Ph.D. degree in the domain of aerospace engineering (Ph.D. thesis: complex adaptive and optimal systems for the Stabilization, Navigation and Control of the Flying Objects). Since 2016 he is an associate professor at the University of Craiova, Electrical, Energetic, and Aerospace Engineering Department. His fields of interest include: the flight control systems, automatic pilots, gyroscopic equipment and systems etc. His scientific experience includes: 7 books/chapters in books; 2 laboratory guidelines; 1 patent; 140 published papers; 17 scientific research grants; 138 citations.

Romulus Lungu was born in Bistrita Nasaud, Romania, in 1952. In 1976 he graduated the University of Craiova, Faculty of Electrotechnics, specialization: automatics and computers. In 1991 he received the Ph.D. degree (aerospace engineering domain). Since 1997 he is a professor at the University of Craiova, Avionics Division. He is the founder of the specialisation board equipments and devices at the University of Craiova and since 2009 he is Ph.D. leader in the domain of aerospace engineering. His interest fields are: automatics of the flying objects, rockets' control, auto-pilots, gyroscopic equipment and systems etc. His scientific experience includes: 13 books/chapters in books; 6 laboratory guidelines; 237 published papers; 22 scientific research grants; 152 citations.